

Received 3 April 2025, accepted 21 April 2025, date of publication 24 April 2025, date of current version 1 May 2025.

Digital Object Identifier 10.1109/ACCESS.2025.3564032



# **A Novel LSTM Architecture for Automatic Modulation Recognition: Comparative Analysis With Conventional Machine Learning** and RNN-Based Approaches

SAM ANSARI<sup>®1</sup>, SOLIMAN MAHMOUD<sup>®2,3</sup>, (Senior Member, IEEE), SOHAIB MAJZOUB<sup>®</sup><sup>2</sup>, (Senior Member, IEEE), EQAB ALMAJALI<sup>®</sup><sup>2</sup>, (Member, IEEE), ANWAR JARNDAL<sup>®</sup><sup>2</sup>, (Senior Member, IEEE), AND TALAL BONNY<sup>®</sup>
<sup>1</sup>Research Institute of Science and Engineering, University of Sharjah, Sharjah, United Arab Emirates

Corresponding author: Soliman Mahmoud (solimanm@sharjah.ac.ae)

**ABSTRACT** The recognition of modulation types in received signals is essential for signal detection and demodulation, with broad applications in telecommunications, defense, and wireless communications. This paper introduces a pioneering approach to automatic modulation recognition (AMR) through the development of a highly optimized long short-term memory (LSTM) network. The proposed framework is engineered to capture intricate temporal dependencies within modulated signals, leveraging a gated architecture that effectively mitigates the vanishing gradient problem. This innovation markedly improves recognition accuracy, particularly in low-SNR conditions where traditional methods are often limited. A defining contribution of this work is the introduction of a novel, adaptive temporal-spectral feature learning mechanism, which seamlessly integrates both temporal and spectral characteristics of the signal. This paradigm eliminates the need for manual feature extraction, enhances interpretability, and significantly boosts classification efficiency. Furthermore, the proposed framework is designed for low-complexity deployment, ensuring its scalability and suitability for next-generation wireless networks and real-time communication systems. The proposed architecture is capable of distinguishing between seven modulation classes: BASK, 4-ASK, BFSK, 4-FSK, BPSK, 4-PSK, and 16-QAM. Performance is evaluated across a broad range of signal-to-noise ratios (SNR), from -10 dB to +30 dB, through extensive simulations. Experimental results demonstrate that the model achieves a recognition accuracy of 99.87% at an SNR of -5 dB, outperforming several conventional machine learning techniques, including multi-layer perceptron (MLP), radial basis function (RBF) networks, adaptive neuro-fuzzy inference systems (ANFIS), decision trees (DT), naïve Bayes (NB), support vector machines (SVM), probabilistic neural networks (PNN), knearest neighbors (KNN), and ensemble learning models, as well as recurrent neural networks (RNNs). Comparative analysis reveals that the proposed framework outperforms conventional machine learning techniques, with accuracy improvements ranging from 1.77% to 34.03% over the best- and worst-performing methods. Additionally, the proposed model achieves a performance gain of 2.02% over the deep learning (DL)-based RNN, further highlighting its superior capability in AMR.

**INDEX TERMS** Automatic modulation recognition, classification, conventional algorithms, deep learning, long short-term memory.

The associate editor coordinating the review of this manuscript and approving it for publication was Mohammad J. Abdel-Rahman.

# I. INTRODUCTION

In modern wireless communication systems, accurate and efficient signal processing is fundamental to ensuring reliable

<sup>&</sup>lt;sup>2</sup>Electrical Engineering Department, University of Sharjah, Sharjah, United Arab Emirates

<sup>&</sup>lt;sup>3</sup>Electrical Engineering Department, Fayoum University, Fayoum 63514, Egypt

<sup>&</sup>lt;sup>4</sup>Computer Engineering Department, University of Sharjah, Sharjah, United Arab Emirates



data transmission. One of the most critical tasks in this domain is automatic modulation recognition (AMR), which plays a key role in both military and civilian applications. In military contexts, AMR enables spectrum surveillance, electronic warfare, and signal intelligence, while in civilian domains, it is crucial for cognitive radio, adaptive communication, and spectrum monitoring [1], [2]. Given the rapid evolution of wireless networks, the need for highly accurate, robust, and efficient AMR methods has become increasingly important.

Over the past few decades, AMR techniques have evolved significantly, driven by the need for improved classification accuracy and real-time adaptability [3], [4], [5], [6], [7]. Traditional AMR methods are broadly classified into decision theory-based and pattern recognition-based approaches. Decision theory-based methods rely on statistical modeling and predefined rules, such as Bayesian inference and the Neyman-Pearson criterion, to classify modulation types [8]. While these methods are mathematically rigorous, they suffer from high computational complexity and limited adaptability in dynamic environments [9]. Pattern recognition-based methods extract discriminative features from received signals—such as normalized amplitude, higher-order statistics, and momentary standard deviation to perform classification [10]. While more flexible than decision-theoretic models, their reliance on manually engineered features makes them prone to errors in complex and noisy conditions, particularly at low signal-to-noise ratios (SNRs) [5].

A major drawback of traditional AMR techniques is their inability to generalize well under diverse channel conditions, where noise, fading, and interference significantly degrade classification accuracy. Additionally, manual feature extraction is computationally expensive and often impractical for modern high-speed communication systems. To overcome the limitations of conventional methods, deep learning (DL)-based AMR approaches have gained significant attention. Unlike traditional techniques, DL models automatically learn hierarchical features from raw signals, eliminating the need for manual feature engineering [11], [12], [13], [14].

Among DL models, convolutional neural networks (CNNs) have shown remarkable success in AMR by treating signals as time-frequency representations and extracting spatial features [15], [16]. Several studies have leveraged CNNs for AMR with promising results. For instance, in [17], time-domain signals are transformed into spectrograms using the short-time Fourier transform (STFT), followed by a CNN for classification. A compact CNN architecture is introduced in [18], where constellation images serve as input to optimize both accuracy and computational efficiency. Additionally, [19] proposes a hybrid CNN model that utilizes grid constellation matrices and contrastive loss functions to improve feature separation.

While CNN-based models have improved modulation classification accuracy, their primary limitation is their

inability to capture temporal dependencies, which are crucial in wireless signal analysis [20], [21]. Since modulated signals exhibit dynamic amplitude and phase variations over time, temporal relationships are critical for robust AMR. However, CNNs are inherently designed for spatial feature extraction and fail to effectively model these dependencies.

Wireless signals are inherently time-dependent sequences, making it essential to incorporate models capable of learning long-term temporal dependencies. However, many existing DL-based AMR methods overlook this aspect, focusing primarily on spatial features [4], [5], [6], [7], [16], [22]. To address this challenge, this paper proposes a novel AMR framework based on an optimized long short-term memory (LSTM) network. LSTMs are specifically designed to handle sequential data, overcoming the vanishing gradient problem in traditional recurrent neural networks (RNNs). Unlike CNN-based models that primarily learn local spatial features, LSTMs effectively capture both short-term and long-term dependencies in modulated signals, making them well-suited for AMR applications.

The proposed LSTM-based AMR model offers several advantages. Unlike CNNs, which focus on spatial patterns, LSTMs learn how modulation characteristics evolve over time, leading to higher classification accuracy in dynamic environments. The model demonstrates strong noise resilience, making it particularly effective in real-world wireless scenarios where traditional methods struggle. Additionally, the optimized LSTM structure ensures reduced computational overhead, facilitating deployment in resource-constrained environments such as next-generation, i.e., beyond fifth-generation (5G) and sixth-generation (6G) wireless networks. This work introduces a state-of-the-art LSTM-based AMR framework, rigorously evaluated against traditional AMR techniques, ensemble learning models, and DL architectures, including RNNs. The key contributions of this paper include the development of a novel LSTM-based AMR model that efficiently captures both spatial and temporal features, overcoming the limitations of CNN-based approaches. The study presents a comprehensive benchmarking analysis against a wide range of AMR techniques, demonstrating the superior classification performance of the proposed model. Extensive experimental validation is conducted, showcasing robust performance across varying SNR levels and complex wireless environments. By integrating deep temporal modeling with efficient neural architectures, this research paves the way for next-generation AMR solutions with enhanced accuracy, adaptability, and realworld applicability.

Building on these foundations, the key contributions of this work are as follows.

 Innovative LSTM-based AMR framework for superior temporal-spectral feature extraction: This work introduces a novel LSTM-based AMR framework designed to capture intricate temporal dependencies in modulated signals with unparalleled precision. By leveraging an optimized gated architecture, the model mitigates the



- vanishing gradient problem and significantly enhances recognition accuracy, particularly under challenging low-SNR conditions, where conventional methods struggle.
- Redefining feature learning with optimized and adaptive temporal-spectral processing: Departing from conventional handcrafted feature extraction, the proposed approach introduces an adaptive feature learning paradigm that seamlessly integrates both temporal and spectral characteristics of signals. This eliminates reliance on manual feature engineering, enhances interpretability, and significantly improves classification efficiency. Moreover, the framework is optimized for low-complexity deployment, ensuring scalability in next-generation wireless networks and real-time communication systems.
- Comprehensive benchmarking and superior performance over traditional and DL architectures: Through a comprehensive comparative analysis against traditional machine learning models, ensemble learning frameworks, and DL-based RNNs, the proposed model demonstrates significant accuracy improvements. Achieving 99.87% accuracy at -5 dB SNR and surpassing the best conventional method by up to 34.03% and the RNN by 2.02%, this work sets a new benchmark for AMR performance, reinforcing its robustness in real-world signal environments.

The remainder of this paper is organized as follows. Section II provides a comprehensive review of related work and state-of-the-art approaches in AMC, highlighting key advancements, methodologies, and their respective strengths and limitations. Section III discusses the selected features and employed algorithms, outlining the foundational assumptions of this study. Section IV elaborates on the methodology of the proposed architecture, providing an in-depth discussion of the algorithm. Section V details the experimental studies, including the simulation and evaluation processes associated with the algorithm. Finally, Section VI presents the conclusions, summarizes the findings, and offers recommendations for future research.

# II. RELATED WORK AND STATE-OF-THE-ART APPROACHES IN AMC

AMC has been extensively studied in the literature, with numerous approaches proposed to enhance classification performance [23], [24], [25], [26], [27], [28], [29], [30], [31], [32]. While early AMC techniques relied on traditional feature-based classification methods, they often suffered from limited accuracy and robustness, particularly in dynamic and noisy environments. Consequently, DL-based solutions have gained prominence due to their ability to automatically extract complex temporal and spectral features from modulated signals, leading to significant performance improvements over conventional methods. A detailed review of the advancements in this field can be found in [33]

and [34]. Figure 1 illustrates a comparison of the performance of traditional methods and DL techniques.

CNNs have emerged as a widely used DL architecture for AMC, demonstrating superior feature extraction capabilities. O'Shea et al. [22], [35], [36], [37] pioneered the application of CNNs for classifying modulation schemes directly from time-domain signal representations, achieving notable improvements in classification accuracy. Subsequent research, such as that by Kulin et al. [38], refined CNN architectures by incorporating domain and phase information, further enhancing classification performance.

Several studies have explored modifications to CNN architectures to improve robustness under real-world conditions. For instance, Yashashwi et al. [39] introduced a signal distortion correction module within a CNN framework to mitigate frequency and phase offsets, leading to improved classification outcomes. Other works, such as [10] and [40], leveraged image-based signal representations, utilizing CNNs to extract discriminative features from eye diagrams and high-frequency radio signals. Peng et al. [41] demonstrated that architectures such as AlexNet and GoogLeNet could effectively process raw modulated signals by transforming them into image representations, particularly under additive white Gaussian noise (AWGN) conditions. However, these methods exhibited performance degradation in complex scenarios involving channel impairments like fading and interference. Addressing this, [42] proposed converting modulated signals into time-frequency representations before applying CNNs, thereby improving classification accuracy under more challenging conditions.

In line with recent advancements in modulation schemes for future communication systems, hexagonal quadrature amplitude modulation (HQAM) has emerged as a promising approach for supporting high data rates and energy efficiency, particularly in 6G networks. The work in [43] propose a simple yet accurate closed-form symbol error probability (SEP) approximation for HQAM constellations, along with tight upper bounds that are especially effective for higher-order constellations ( $M \ge 256$ ). They also introduce a low-complexity detection scheme with efficiency comparable to maximum likelihood detection (MLD) but with reduced computational complexity  $(O(\log \sqrt{M}))$ . The study provides valuable insights into the performance of HQAM and its potential benefits in practical systems, reinforcing its relevance for future modulation schemes in AMR systems.

A recent study in [28] addressed the challenge of AMC under phase imperfections (PI) and imperfect channel state information (CSI), which significantly degrade classification accuracy in real-world wireless environments. To mitigate these issues, Oikonomou et al. proposed a CNN-based framework that applies a polar transformation to the received signals, enhancing robustness against PI. Additionally, they introduced an asymmetric kernel dimension modification in CNN layers, optimizing feature extraction based on the geometry of modulated schemes. Simulation results



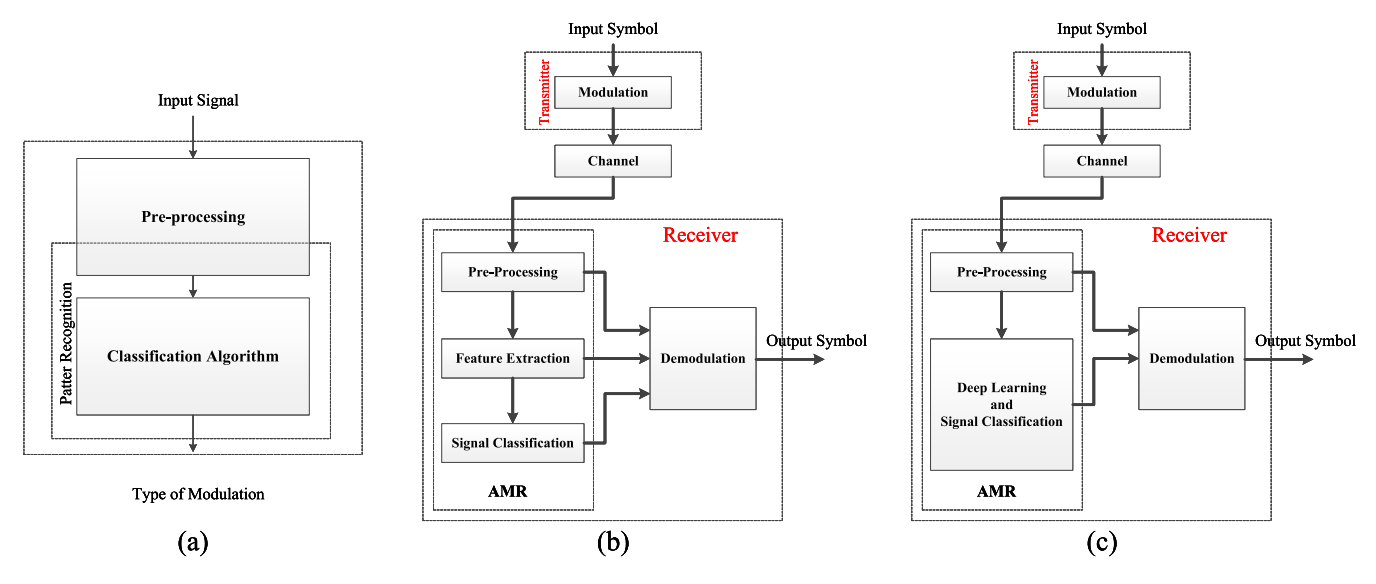


FIGURE 1. (a) An illustration of modulation recognition systems. (b) Simplified block diagram illustrating automatic modulation recognition in traditional methods, which necessitate feature extraction. (c) Block diagram of deep neural networks, representing end-to-end approaches where feature extraction is performed automatically within the layers of the network.

demonstrated that this approach effectively improves AMC accuracy, even under severe PI conditions, while maintaining low computational complexity. Notably, the study also challenged the assumption that more complex CNN architectures always yield superior performance, showing that the proposed method enables simpler models to outperform deeper networks in PI-affected scenarios. These findings highlight the potential of tailored CNN modifications to enhance AMC performance without increasing system overhead.

RNNs, particularly LSTM networks, have gained traction in AMC due to their ability to capture temporal dependencies in sequential data. Rajendran et al. [44] utilized LSTMs to classify modulation schemes, emphasizing domain and phase information. However, LSTM-based models often struggle with capturing spatial features, which can limit their overall classification accuracy. To address these limitations, researchers have explored hybrid CNN-LSTM architectures. The work in [22] introduced a CNN-LSTM-based deep neural network (CLDNN) that effectively captured both spatial and temporal signal characteristics, achieving high classification accuracy using only in-phase and quadrature (I/Q) signal representations. Similarly, the hybrid LSTM architecture in [45] attained a peak classification accuracy of 95% at 18 dB signal-to-noise ratio (SNR), demonstrating the efficacy of combining LSTMs with other DL models.

Recent advancements have further refined hybrid architectures by integrating LSTM networks with residual networks (ResNet) to improve feature extraction and mitigate issues such as gradient vanishing and overfitting [46]. This approach achieved an accuracy of 92% at 18 dB SNR, outperforming standalone CNN and CLDNN models. While LSTM

networks remain a powerful tool for AMC, their effectiveness is often enhanced when combined with other architectures that compensate for their limitations.

Recognizing the strengths and weaknesses of individual DL models, hybrid architectures have emerged as a promising direction for AMC [46], [47], [48], [49], [50], [51], [52], [53], [54]. By leveraging the complementary strengths of multiple neural network models, hybrid approaches have demonstrated improved classification robustness in diverse signal environments. For instance, [55] proposed a dual CNN-based framework, where a signal-based CNN (SBCNN) was used to extract features from raw time-domain signals before transforming them into heat maps processed by an image-based CNN (IBCNN). This hybrid approach exhibited superior classification accuracy, particularly in low-SNR conditions. Similarly, [47] introduced a dual-stream model combining CNNs and LSTMs to capture both spatial and temporal characteristics of modulated signals, yielding higher accuracy than traditional CNN-based solutions. Ke and Vikalo [48] further advanced hybrid AMC models by integrating LSTMs with denoising autoencoders (AEs) to enhance feature extraction under noisy conditions. Meanwhile, Wang et al. [50] introduced a novel CNN-transformer-graph neural network (CTGNet) model, leveraging transformers' attention mechanisms and graph neural networks' (GNNs) structural learning capabilities to improve AMC performance.

Transformers, known for their ability to capture long-range dependencies in data, have recently been explored for AMC applications. The deep hybrid transformer network (DH-TR) proposed in [56] combines convolutional, recurrent, and transformer-based modules to extract both local and global signal features. By integrating a convolutional stem for initial feature extraction, a gated recurrent unit (GRU) for sequential



TABLE 1. Comparison of AMC techniques in the literature.

Ref.	Approach	Key Contributions	Strengths	Weaknesses	
[35], [37], [10], [39], [41]	CNN-Based AMC	Utilizes convolutional layers to extract spatial features from I/Q data or image representations.	Strong feature extraction capabilities; Works well with image-based signal representations.	Struggles with temporal dependencies in time-series data; Performance degrades under complex channel conditions.	
[28]	CNN with Polar Transformation	Addresses Pland CSI impairments by applying a polar transformation before CNN processing.	Enhances AMC accuracy under severe PI conditions; More robust to phase noise and synchronization errors.	Requires additional preprocessing step; Performance depends on transformation quality.	
[44], [45], [22]	LSTM-Based AMC	Uses recurrent layers to capture temporal dependencies in modulated signals.	Excellent for sequential data analysis; Effective in handling time-varying signals.	Weak in spatial feature extraction; Higher training complexity.	
[22], [45]	Hybrid CNN-LSTM (CLDNN)	Combines CNNs for spatial features and LSTMs for temporal dependencies.	Captures both spatial and temporal features; Achieves better accuracy than standalone CNN or LSTM models.	High computational cost; Requires complex hyperparameter tuning.	
[39]	CNN with Signal Distortion Correction	Introduces pre-processing modules to correct frequency and phase offsets before classification.	Robust against phase/frequency distortions; Improves performance in real- world conditions.	Still sensitive to complex noise conditions; Additional preprocessing overhead.	
[48]	Denoising Autoencoder with LSTM	Uses autoencoders to remove noise before LSTM-based classification.	Enhanced robustness to noise and channel impairments; More reliable classification in low-SNR environments.	Increased model complexity; Requires significant computational resources.	
[42]	CNN with Time-Frequency Representations	Converts modulated signals into spectrograms for improved feature extraction.	Better classification under fading and interference; Leverages CNN's strengths in image processing.	Increased preprocessing complexity; Computationally intensive.	
[46]	Hybrid CNN- ResNet-LSTM	Integrates ResNet with LSTM to improve feature extraction and address vanishing gradient issues.	More efficient training; Outperforms standalone CNN and CLDNN models.	High memory and computational requirements.	
[51], [52]	CNN- Transformer Hybrid	Uses attention mechanisms to capture long-range dependencies in modulation signals.	Excels in feature selection; Improved interpretability.	Computationally expensive; Requires large training datasets.	
[56]	Transformer- Based AMC (DH-TR)	Combines CNN, GRU, and transformer to extract local and global signal features.	Achieves state-of-the-art accuracy; Adapts well to diverse signal environments.	High computational cost; Challenging for real-time deployment.	
[50]	Graph Neural Networks (GNN) with Transformers (CTGNet)	Uses GNNs to model signal dependencies while transformers capture attention-based features.	Superior classification performance; Robust against channel impairments.	Requires extensive computational resources; Model complexity may hinder real-time deployment.	

pattern recognition, and a transformer branch for capturing long-term dependencies, the DH-TR model achieved state-of-the-art performance across multiple benchmark datasets. However, despite its high accuracy, the model remains computationally intensive, limiting its deployment in real-time and resource-constrained environments.

Other studies have investigated transformer-based hybrid models, such as CNN-transformer networks, to improve feature extraction efficiency and robustness under real-world signal conditions [51], [52]. These approaches have shown promise in addressing challenges related to PI and CSI inaccuracies, which are critical factors in next-generation wireless networks. Table 1 provides a comprehensive comparison of existing AMC techniques, highlighting their key contributions, strengths, and limitations. This comparison

highlights the trade-offs between various DL models and hybrid approaches, emphasizing the need for more efficient and robust solutions in real-world communication environments.

Despite the significant advancements in DL-based AMC, several challenges remain. While CNNs excel at extracting spatial features, they struggle with modeling temporal dependencies in dynamic signal environments. Conversely, LSTMs effectively capture temporal relationships but lack the ability to fully leverage spatial information. Hybrid approaches that integrate CNNs, LSTMs, and transformers have demonstrated improvements in classification accuracy, yet they often introduce increased computational complexity, making real-time deployment challenging. While recent advancements in AMC have leveraged DL models such as CNNs,



LSTMs, and hybrid architectures, several challenges persist in real-world applications, particularly in environments with low SNR, PI, and imperfect CSI. Notably, while architectures like deep hybrid transformer networks offer impressive performance, their computational intensity poses challenges for real-time deployment, particularly in resource-constrained scenarios. Furthermore, existing approaches typically rely on either handcrafted feature extraction or rigid DL pipelines that may fail to adapt dynamically to diverse, unpredictable signal environments. The inherent trade-offs between model complexity, accuracy, and computational efficiency in these methods remain inadequately addressed, particularly in the context of next-generation wireless systems that demand both high performance and low computational overhead. The existing models are primarily optimized for benchmark datasets, leaving uncertainties regarding their generalizability to real-world radio signal conditions, including varying levels of interference, multipath fading, and channel impairments. Additionally, balancing classification accuracy with computational efficiency remains an open problem, particularly for resource-limited applications in B5G and 6G networks.

This work directly addresses the aforementioned research gaps by introducing an innovative LSTM-based AMR framework that offers superior temporal feature extraction capabilities. Unlike traditional methods that rely on static feature extraction, our approach utilizes an optimized gated architecture within the LSTM framework, which effectively mitigates the vanishing gradient problem and enhances the model's ability to capture complex temporal dependencies. This architecture is especially valuable under challenging low-SNR conditions, where previous methods, including DL approaches, struggle to maintain accuracy.

In addition, this study redefines feature learning by integrating both temporal and spectral characteristics of modulated signals in an adaptive manner. This removes the reliance on conventional handcrafted feature extraction techniques, which can be both time-consuming and prone to error. The proposed adaptive learning paradigm ensures that the model can dynamically adjust to varying signal conditions, enhancing both interpretability and classification efficiency. Importantly, the framework is optimized for low-complexity deployment, making it suitable for real-time communication systems and scalable for next-generation wireless networks, which is a critical advancement over previous, more computationally demanding models such as those based on hybrid transformers.

# **III. SELECTED FEATURES AND EMPLOYED ALGORITHMS**

This study critically evaluates the performance of traditional algorithms in comparison to a novel DL-based approach. The traditional algorithms function on extracted features, relying on no prior information about the received signal as it traverses an additive white Gaussian noise (AWGN) channel. Within this communication framework, the transmitted signal is modulated and subsequently blended with Gaussian noise, entering the receiver block devoid of any transmitter-specific

knowledge. For communication systems, the modulated input signal can be represented mathematically as:

$$z(t) = \tilde{s}(t)e^{j(2\pi f_c t + \phi_c)} + n(t), \tag{1a}$$

where

$$\tilde{s}(t) = a(t)e^{j[2\pi f(t)t + \phi(t)]},\tag{1b}$$

where  $f_c$  denotes the carrier frequency,  $\phi_c$  represents the carrier phase, n(t) signifies the Gaussian white noise, and  $\tilde{s}(t)$  indicates the modulated signal s(t). The parameters a(t), f(t), and  $\phi(t)$  correspond to the amplitude, frequency, and phase of the signal, respectively. The assumptions guiding this study, along with comparisons to prior work [4], [6], [57], [58], are succinctly summarized in Table 2.

**TABLE 2.** Parameters and assumptions of signals employed in simulation datasets.

Index	Parameter	Value
1	Sampling Frequency $(f_s)$	1200 KHz
2	Carrier Frequency $(f_c)$	150 KHz
3	Symbol Rate $(r_s)$	12.5 KHz
4	Number of Modulations	7
5	Total Samples	$7 \times 3600$
6	Continuous Wavelet Transform (CWT)	Haar function with 64 scale values

This analysis categorizes the modulations into seven distinct classes: binary amplitude-shift keying (BASK), 4-ary amplitude-shift keying (4-ASK), binary frequency-shift keying (BFSK), 4-ary frequency-shift keying (4-FSK), binary phase-shift keying (BPSK), 4-ary phase-shift keying (4-PSK), and 16-ary quadrature amplitude modulation (16-QAM). The features utilized in this research are briefly outlined in the following Section. Through meticulous processing of the input data, distinctive characteristics of the modulation schemes are extracted and employed in the learning processes of traditional algorithms.

# A. UTILIZED FEATURES

AMR techniques leverage a variety of features to effectively distinguish between modulation types. A pivotal question arises: which features are most effective in maximizing classification accuracy. Furthermore, considering the real-time demands of modulation recognition, it is imperative to identify features that optimize processing speed. Previous studies grounded in traditional learning methodologies have explored an array of features [3], [57], [59], [60], [61], [62]. This study highlights specific features identified in previous work [4], [6], [58], which are elaborated upon as follows.

The second-order moment of the non-linear component of the instantaneous phase is the first feature utilized in the AMR framework. The mathematical representation of this attribute is defined as:

$$M_{\phi_{NL}} = \frac{1}{N_s} \sum_{i=1}^{N_s} \phi_{NL}^2(i),$$
 (2a)



where

$$\phi_{NL}(i) = \frac{\phi(i)}{\bar{\phi}} - 1, \tag{2b}$$

where  $N_s$  represents the number of symbols,  $\phi_{NL}(i)$  denotes the normalized non-linear component of the instantaneous phase,  $\phi(i)$  indicates the instantaneous phase, and  $\bar{\phi}$  is the mean phase. Signals modulated by ASK lack information in their instantaneous phase, resulting in the lowest computed values of  $M_{\phi_{NL}}$  compared to other modulation types. This characteristic effectively distinguishes between BASK, 4-ASK modulations, and other modulation schemes such as QAM, PSK, and FSK.

The second feature employed in this study is a spectrumbased characteristic, defined as follows:

$$\sigma_z^2 = \frac{1}{N_s} \sum_{i=1}^{N_s} \left( Z(i) - \frac{1}{N_s} \sum_{j=1}^{N_s} Z(j) \right)^2,$$
 (3)

where Z(i) represents the discrete-time Fourier transform (DTFT) of the received signal. This feature effectively differentiates ASK and QAM from other digital modulation schemes, including PSK and FSK, which do not convey amplitude-related information.

The third attribute incorporated into the proposed AMR system is the mean value of the power spectral density of the normalized instantaneous amplitude of the received signal segment, expressed as:

$$\gamma = \frac{1}{N_s} \sum_{i=1}^{N_s} |A_{cn}(i)|^2,$$
 (4a)

where

$$a_{cn}(i) = \frac{a(i)}{m_a} - 1,$$
 (4b)

and

$$m_a = \frac{1}{N_s} \sum_{i=1}^{N_s} a(i),$$
 (4c)

where  $A_{cn}$  refers to the DTFT of the normalized instantaneous amplitude,  $a_{cn}(i)$  signifies the normalized instantaneous amplitude, and  $m_a$  is the mean instantaneous amplitude. This characteristic enables the proposed models to differentiate 4-ASK modulation from BASK.

As the fourth feature, the standard deviation of the normalized non-linear component of the instantaneous phase, which encompasses phase-related information, is analyzed. The mathematical formulation for extracting this attribute is given by:

$$\sigma_{dp} = \sqrt{\frac{1}{N_s} \sum_{i=1}^{N_s} \phi_{NL}^2(i) - \left(\frac{1}{N_s} \sum_{i=1}^{N_s} \phi_{NL}(i)\right)^2}.$$
 (5)

This characteristic is utilized to distinguish PSK from quadrature PSK (QPSK) in hierarchical classifiers.

The fifth and sixth features of the framework involve the continuous wavelet transform (CWT), which facilitates time-frequency analysis and is mathematically defined as:

$$CWT_{\psi}x(\tau,s) = \psi_{x}(\tau,s) = \int_{-\infty}^{\infty} x(t)\psi_{\tau,s}^{*}(t)dt, \qquad (6a)$$

where

$$\psi_{\tau,s}(t) = \frac{1}{\sqrt{|s|}} \psi\left(\frac{t-\tau}{s}\right),\tag{6b}$$

where  $\tau$  as the translation parameter, s as the scale parameter, and  $\psi^*(t)$  representing the complex conjugate of  $\psi(t)$ . This method calculates the correlation between the wavelet transform of the received signal and the predefined patterns within the system. For the wavelet transform simulations, the Haar function is employed. By comparing the calculated CWT against templates for BASK and BFSK, the system effectively distinguishes among BPSK, QPSK, BFSK, and 4-FSK modulations.

#### B. CONVENTIONAL MACHINE LEARNING ALGORITHMS

A critical element of AMR lies in the utilization of classifiers based on machine learning methodologies. This work employs eight distinct machine learning algorithms, instantiated across nine models. The first algorithm is the multi-layer perceptron (MLP), which utilizes the backpropagation technique during its training phase. The second algorithm is the radial basis function (RBF), characterized by a three-layer architecture that incorporates Gaussian functions in the hidden layer. The third algorithm, adaptive neuro-fuzzy inference system (ANFIS), stands out as a pivotal neuro-fuzzy methodology.

The fourth algorithm employed is the decision tree (DT), a highly regarded method in data mining that employs entropy measures to identify optimal features. The fifth algorithm, naïve Bayes (NB), leverages simple probabilistic classifiers based on prior distributions. The sixth algorithm, k-nearest neighbors (KNN), categorizes data based on proximity metrics. The seventh algorithm is the probabilistic neural network (PNN), a variant of RBF networks characterized by a four-layer structure dedicated to computing the probability density function (PDF) for each class.

The eighth algorithm is the support vector machine (SVM), implemented using both one-against-all (OAA) and one-against-one (OAO) strategies to optimize classification accuracy. The ninth approach involves ensemble learning, which combines multiple weak learners or base models, enhancing performance through collective learning. Detailed descriptions of each algorithm are omitted, though parameters utilized in each model are presented in Section V.

# C. DEEP LEARNING MODEL

In this study, a RNN is employed as a DL approach to AMR. RNNs are well-regarded for their ability to model sequential



data, leveraging recurrent connections to capture temporal dependencies effectively. This makes them highly suitable for AMR tasks, particularly in low SNR scenarios [63]. As part of a diverse and comprehensive comparison, RNN performance is evaluated alongside traditional machine learning algorithms and advanced DL techniques. RNN's performance is further compared with both conventional machine learning algorithms and the proposed model to highlight its relative strengths and limitations in AMR tasks. This inclusion allows for a comprehensive evaluation of DL techniques in the context of AMR. Detailed implementation parameters of the RNN model are provided in Section V.

#### IV. METHODOLOGY OF THE PROPOSED ARCHITECTURE

In recent years, various CNN models have been developed to enhance the efficacy of AMR. Modulation signals are typically modeled as continuous time-varying codes, with the amplitude and phase of different modulation types following specific statistical distribution laws over time. However, many existing CNN architectures neglect these temporal relationships, highlighting the necessity for algorithms that effectively incorporate these inherent characteristics of modulation signals during the learning process.

RNN, LSTM networks, and gated recurrent units (GRUs) represent three prominent architectures within the realm of recurrent neural networks. RNNs are particularly suited for tasks involving sequential data, such as speech recognition and natural language processing (NLP). Unlike traditional deep networks like CNNs, which are structured as feed-forward networks processing inputs in a singular direction, RNNs maintain an internal memory. This recurrent architecture allows RNNs to apply the same function to each input while enabling the current output to depend on prior computations. After generating an output, this information is fed back into the network, facilitating a decision-making process that takes into account both the current input and the previously learned outputs.

LSTM networks specifically address the limitations associated with conventional RNNs, notably the vanishing gradient problem, by replacing the recurrent layer with an LSTM block [64]. LSTMs incorporate internal mechanisms known as gates, which regulate the flow of information and determine which data in a sequence are essential for retention and which can be discarded. This capability enables the network to transmit critical information throughout the sequence, ensuring the desired output is achieved. Figure 2 illustrates a comparative analysis of inputs and outputs within the RNN and LSTM architectures.

In the LSTM architecture, the hidden state input is denoted by h, while C represents the cell state—a crucial component often referred to as long-term memory. This memory possesses two key attributes: the ability to delete information, i.e., forgetting, and the capacity to incorporate new information i.e., remembering. The LSTM model is trained through backpropagation. An LSTM network

incorporates three essential gates, illustrated in Figure 3: the input or update gate, the forget gate, and the output gate.

The following equations elucidate the principles underlying the LSTM methodology [64]:

$$f_t = \sigma(W_f \cdot [h_{t-1}, x_t] + b_f), \tag{7a}$$

$$i_t = \sigma(W_i \cdot [h_{t-1}, x_t] + b_i), \tag{7b}$$

$$\bar{C}_t = tanh(W_C \cdot [h_{t-1}, x_t] + b_C), \tag{7c}$$

$$C_t = f_t \cdot C_{t-1} + i_t \cdot \bar{C}_t, \tag{7d}$$

$$o_t = \sigma(W_o \cdot [h_{t-1}, x_t] + b_o), \tag{7e}$$

$$h_t = o_t \cdot tanh(C_t), \tag{7f}$$

where  $f_t$  is the forget gate activation,  $i_t$  indicates the input gate activation,  $x_t$  represents the current input,  $\bar{C}_t$  is the candidate cell state,  $C_t$  is the current cell state,  $o_t$  is the output gate activation,  $h_t$  is the current hidden state. The parameters  $W_f$ ,  $W_t$ ,  $W_c$ ,  $W_o$  are the weight matrices associated with the forget, input, candidate, and output gates, respectively. Moreover,  $b_f$ ,  $b_i$ ,  $b_C$ ,  $b_o$  are the bias vectors for the respective gates,  $\sigma$  denotes the sigmoid activation function, and tanh is the hyperbolic tangent activation function. These equations collectively describe the LSTM's mechanism for maintaining and updating information over time, enabling it to learn long-term dependencies in sequential data.

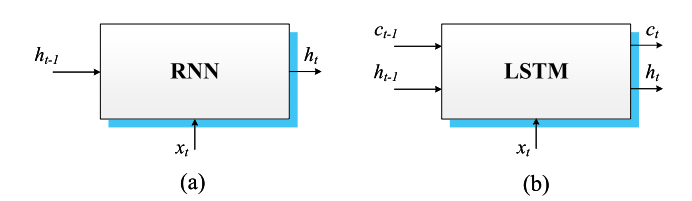


FIGURE 2. Comparative analysis of input and output dimensions in RNN and LSTM architectures.

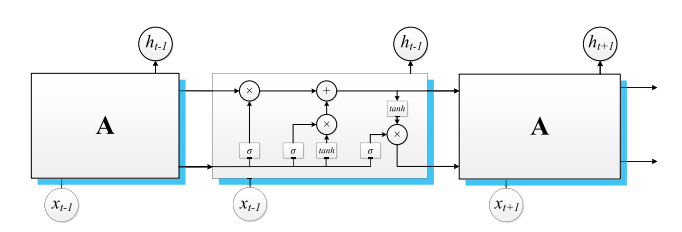


FIGURE 3. Internal structure of LSTM network modules.

LSTMs effectively mitigate the risk of gradient explosion, as all functions and their derivatives remain constrained between zero and one. In contrast, older RNN architectures link each state to the previous one through nonlinear mappings, such as *tanh*, resulting in substantial gradient decay due to repetitive matrix multiplications. The memory cells in LSTMs, however, exhibit a relatively low decay rate at each time step, governed by first-order difference equations.

The architecture of the proposed LSTM model is meticulously designed to address the complex challenges of AMR



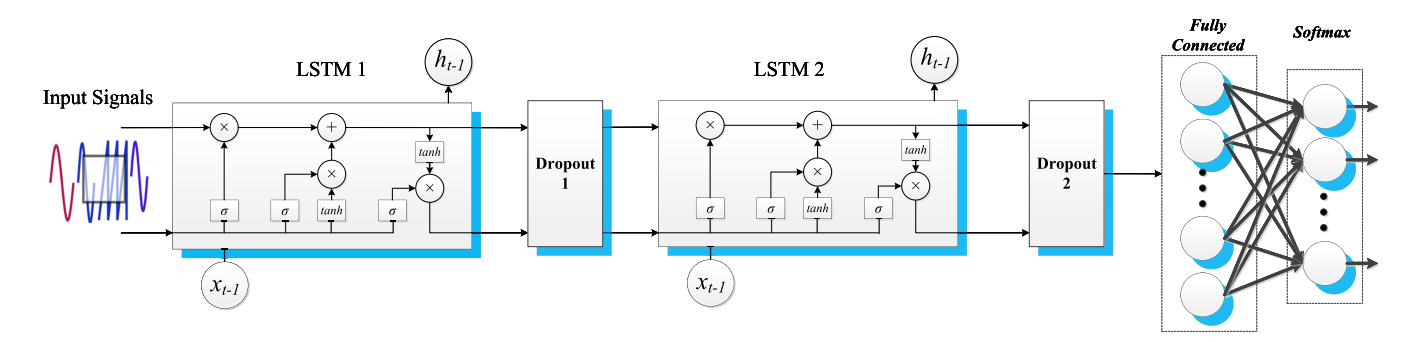


FIGURE 4. Architecture of the proposed model.

under diverse signal conditions. As depicted in Figure 4, the model integrates a sequential flow of LSTM blocks, dropout layers, fully connected dense layers, and a final Softmax layer, each playing a critical role in ensuring the model's robustness and accuracy.

At the core of the architecture is the LSTM layer, which comprises 100 hidden units. Each LSTM cell is structured to manage long-term dependencies in sequential data by incorporating a combination of three gates: the input gate, forget gate, and output gate. These gates regulate the flow of information through the cell state, effectively addressing the vanishing gradient problem inherent in traditional RNNs. The cell state acts as a memory conveyor, selectively retaining or discarding information over long time sequences.

Following the LSTM block, a dropout layer with a rate of 0.2 is incorporated to prevent overfitting. Dropout layers randomly deactivate neurons during training, introducing stochasticity that enhances the model's generalization capability. The fully connected dense layers act as feature aggregators, transforming the sequential data representations from the LSTM into a higher-dimensional space suitable for classification. These layers ensure that temporal dependencies captured by the LSTM are utilized effectively for decision-making.

The Softmax layer at the output serves as the final classification stage. While alternatives like Entmax exist, Softmax remains a widely adopted choice due to its simplicity, efficiency, and well-established performance in similar tasks. By producing a normalized probability distribution across modulation classes, the Softmax function facilitates precise multi-class classification. The mathematical model,  $S_i = \sum_i e^{z_i} e^{z_i}$ , ensures clear distinctions between classes.

To optimize the performance, the model employs the adaptive moment estimation (Adam) optimizer, which combines the advantages of both momentum-based and adaptive learning rate methods, resulting in faster and more stable convergence. Training is conducted using a mini-batch size of 32 for a maximum of 30 epochs, ensuring computational efficiency while achieving high accuracy. The cross-entropy loss function is utilized to minimize classification errors, and ReLU activation is employed throughout the network to enhance gradient propagation and training stability.

Hyperparameter optimization is performed through an extensive grid search combined with evolutionary search techniques. This allowed fine-tuning of critical parameters, including the number of hidden units, learning rate, and dropout rate. The resulting architecture comprises 840,400 trainable parameters, balancing computational efficiency and representational power. To ensure robust and reliable performance evaluation, the model incorporates M-fold cross-validation across 30 iterations. This validation strategy reduces the impact of dataset partitioning bias and ensures consistent performance metrics.

Key features of the proposed LSTM model include:

- Hyperparameter tuning aimed at achieving optimal accuracy, conducted through comprehensive search methodologies complemented by evolutionary search techniques for initial point optimization.
- A total of 100 hidden units, employing the Adam optimizer, resulting in a total of 840,400 parameters within the network.
- The activation function utilized throughout the network is ReLU, which promotes faster convergence during stochastic gradient descent (SGD) and alleviates gradient propagation issues. The softmax function, expressed as  $S_i = \sum_j e^{z_j} e^{z_i}$ , is employed in the final layer.

Algorithm 1 outlines the step-by-step procedure for training the proposed LSTM-based modulation classification model, including the preprocessing steps, feature extraction using the CWT, model architecture consisting of LSTM layers with dropout for regularization, and final classification through a Softmax output. Additionally, it incorporates hyperparameter optimization and model evaluation through cross-validation, ensuring robust performance under varying signal conditions.

#### V. EXPERIMENTAL STUDIES

This section presents a comprehensive evaluation of the proposed algorithm through meticulously designed simulations. All experiments are conducted using MATLAB 2024a, leveraging the capabilities of the neural network toolboxes on a personal computer equipped with a Intel(R) Core(TM) Ultra 125U 1.30 GHz and 16.0 GB of RAM. The simulations



# Algorithm 1 LSTM-Based Modulation Classification

- 1: **Input:** Training dataset  $\mathcal{D}_{train}$ , testing dataset  $\mathcal{D}_{test}$
- 2: Output: Classification model and accuracy
- 3: Initialize:
- 4: LSTM model with 100 hidden units
- 5: Dropout rate = 0.2, Adam optimizer, ReLU activation, softmax output
- 6: Set batch size = 32, epochs = 30, learning rate  $\alpha$
- 7: Preprocessing:
- 8: **for** each signal in  $\mathcal{D}_{train}$  **do**
- 9: Add noise (AWGN) to simulate real-world conditions
- 10: Normalize features to ensure consistent scale
- 11: Apply CWT, i.e., optimized and adaptive temporalspectral, for feature extraction with Haar wavelet
- 12: end for
- 13: **for** each signal in  $\mathcal{D}_{test}$  **do**
- 14: Normalize features
- 15: Apply CWT for feature extraction
- 16: end for
- 17: Model Architecture:
- 18: LSTM with 100 hidden units, followed by a Dropout layer
- Dense layers for feature aggregation and Softmax output for classification
- 20: **Training:**
- 21: **for** epoch = 1 to epochs **do**
- 22: **for** batch in  $\mathcal{D}_{train}$  **do**
- Perform forward pass and compute loss (crossentropy)
- 24: Backpropagate error and update weights using Adam optimizer
- 25: end for
- **26**: **end for**
- 27: Evaluation:
- 28: Evaluate model on validation set for accuracy
- 29: Test model on  $\mathcal{D}_{test}$  and compute final accuracy
- 30: Optimization:
- 31: Perform grid search or evolutionary search for hyperparameter tuning
- 32: **Output:** Trained model and performance metrics (accuracy, precision, F1-score, and confusion matrix)

model a real-world communication channel characterized by AWGN. In this context, the transmitted signal is modulated at the sender's end and subsequently mixed with noise upon traversing the channel, entering the receiver block devoid of any prior knowledge about the sender.

# A. DATASET AND PREPROCESSING

To ensure the robustness, reproducibility, and generalizability of the model, a carefully constructed real-world dataset comprising modulated signals collected from communication systems operating under varying SNR conditions is utilized. The signals are generated and processed using the MATLAB software environment, with key parameters set as follows: carrier frequency of 150 kHz, a sampling rate of 1.2 MHz, and a symbol rate of 12.5 kHz. These settings are representative of typical communication systems, ensuring that the dataset reflects practical conditions encountered in real-world scenarios.

To extract critical features, the CWT with the Haar wavelet function, featuring 64 scale values, is employed. This approach enables efficient capture of time-frequency domain features, such as power spectral density, phase characteristics, and signal amplitudes, which are crucial for distinguishing between different modulation types. The CWT is applied to the generated signals, ensuring that relevant temporal dependencies and modulation-specific features were preserved.

After applying the AWGN channel to the signals, corrupted versions are created to simulate real-world noise conditions. These noisy signals are fed into the model to extract features and perform modulation classification. To guarantee the reliability and reproducibility of the results, two independent datasets for training and testing are generated. Each modulation type comprises 3600 realizations, covering varying SNR levels from  $-5~{\rm dB}$  to  $+30~{\rm dB}$ . This results in a total of 25,200 training samples. For the testing phase, SNR values ranging from  $-10~{\rm dB}$  to  $-6~{\rm dB}$  are added, extending the cumulative SNR range from  $-10~{\rm dB}$  to  $+30~{\rm dB}$ . This ensures the model's ability to generalize across diverse noise conditions, making it robust and applicable to practical AMR scenarios.

Additionally, the dataset generation process follows well-established protocols from previous research, as demonstrated in [4], [6], [58], and [65], ensuring consistency and validation of the proposed framework. The use of real-world data, combined with the rigorous preprocessing steps and feature extraction techniques, ensures that the model is both reliable and reproducible, contributing to the advancement of AMR research.

As illustrated in Figure 5, the variation of selected features with respect to SNR across different modulation schemes is examined to facilitate AMR. The features utilized in this study were introduced and briefly examined earlier in the system model and the feature selection process in Section III. As depicted in Figure 5a, the second-order moment of the non-linear component of the instantaneous phase (denoted as  $M_{\phi_{NI}}$ ), representing the first feature, yields the lowest values for ASK-modulated signals. This feature proves particularly effective in distinguishing ASK modulation from other modulation schemes. Figure 5b highlights the ability of the spectrum-based feature  $\sigma_z^2$  to accurately differentiate between ASK and QAM modulations, while also effectively distinguishing them from other digital modulation types such as PSK and FSK, which do not contain amplitude-related information.

The AMR models developed in this work rely on the mean value of the power spectral density of the



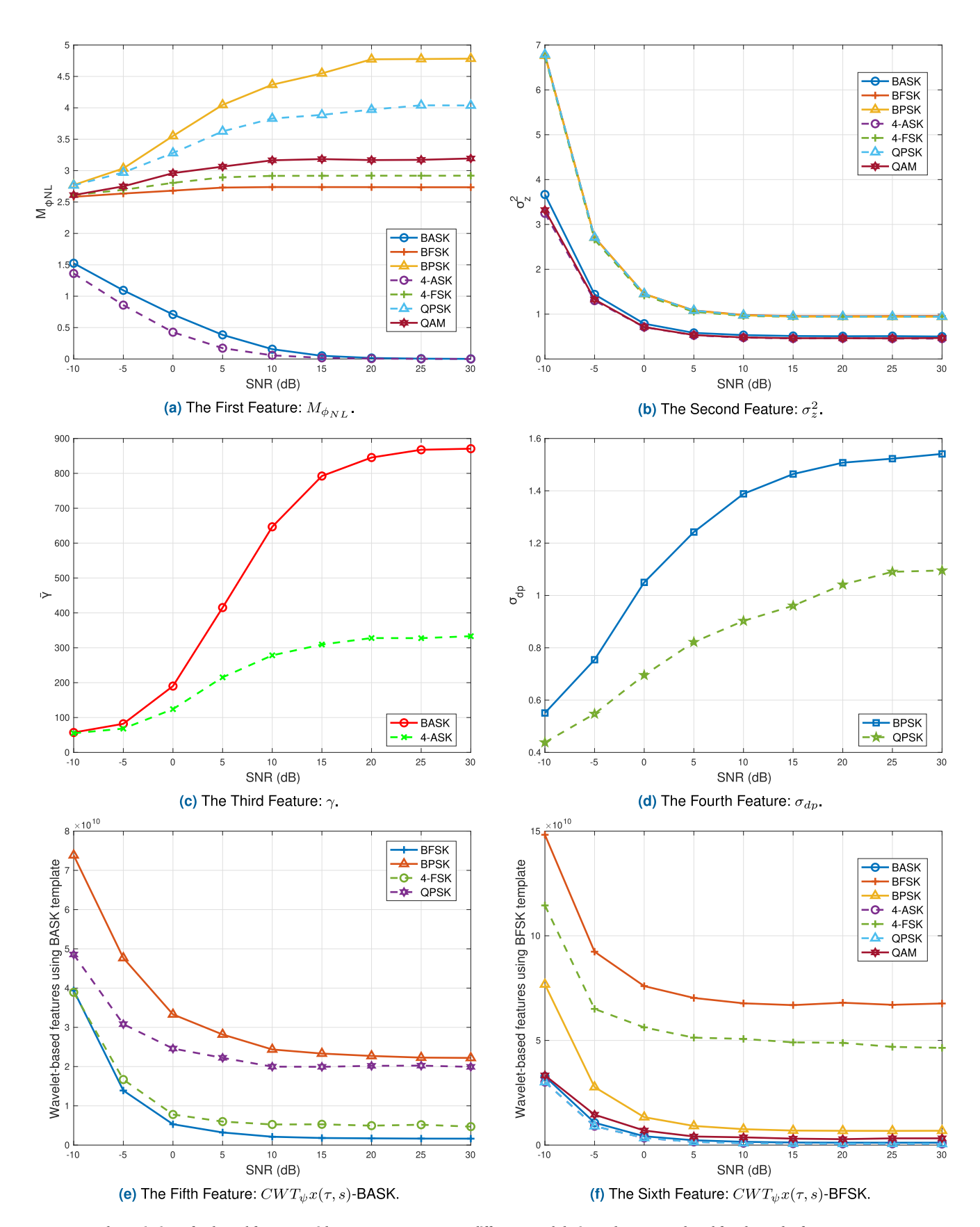


FIGURE 5. The variation of selected features with respect to SNR across different modulation schemes, analyzed for the task of AMR.



normalized-centered instantaneous amplitude of the intercepted signal segment  $(\gamma)$ , as shown in Figure 5c. This feature is instrumental in distinguishing 4-ASK modulations from BASK. Furthermore, Figure 5d demonstrates the use of the standard deviation of the normalized-centered nonlinear component of the direct instantaneous phase  $(\sigma_{dp})$  to differentiate between PSK and QPSK modulations in hierarchical classification systems. Finally, Figures 5e and 5f illustrate how the CWT-based features, i.e.,  $CWT_{\psi}x(\tau,s)$ , enhance the model's ability to identify modulation schemes such as BPSK, QPSK, BFSK, and 4-FSK.

#### B. RESULTS AND PERFORMANCE EVALUATION

A non-ideal channel model with Gaussian noise has been employed, as summarized in Table 2, which outlines the parameters of the utilized signal. Furthermore, Table 3 presents the assumptions related to the parameters of the simulation algorithms, outlining the key values and settings used in the experimental setup. Hyperparameter optimization for all models presented in this work is performed using a rigorous and systematic approach to ensure optimal performance for each model. The hyperparameters of the selected models are fine-tuned using a combination of grid search, genetic algorithm (GA), and particle swarm optimization (PSO), which are well-established techniques for efficiently navigating large search spaces and identifying optimal configurations [4], [6]. These methods are renowned for their effectiveness in achieving high accuracy and robustness in machine learning models.

Additionally, a trial-and-error approach is employed to further refine the hyperparameters, enabling the identification of configurations that maximize accuracy, enhance generalization, and mitigate the risk of overfitting. This comprehensive optimization process underscores the validity of the comparative analysis by ensuring that the models are rigorously tuned for peak performance. To ensure robust evaluation, 10-fold cross-validation is implemented across 30 iterations, with results averaged to enhance reliability. The average error is computed using (8), ensuring consistency with the graphical representations [6]:

$$\bar{\varepsilon} = \frac{1}{P} \sum_{i=1}^{P} \left( \frac{1}{M} \sum_{j=1}^{M} \text{Error\_Fold}_j \right).$$
 (8)

Figure 6 showcases the simulation outcomes across various SNR percentages. The results reveal a signal-to-noise variation spanning from  $-10\,\mathrm{dB}$  to  $+30\,\mathrm{dB}$  for all tested algorithms. Notably, as SNR increases, the accuracy improves significantly, surpassing 94% for numerous algorithms when the SNR exceeds zero. In addition, Figure 7, a zoomed-in version, focuses on the range from -10 to 0 dB, allowing for a more detailed examination of the relevant features within this narrower range. For a detailed comparative analysis, specific results corresponding to designated SNR levels are summarized in Table 4.

**TABLE 3.** Assumptions pertaining to the parameters of the simulation algorithms.

Index	Architecture	Parameters	Values	
1	KNN	K in KNN	5	
2	PNN	Smoothing in PNN	0.1	
		Topology in MLP	[7-20-6]	
3	MLP	LR in MLP	0.2	
		Epochs in MLP	80	
		Neurons in RBF	300	
4	RBF	Spread in RBF	0.9	
		MSE in RBF	0.1	
5	ANFIS	FIS in ANFIS	genfis2	
		Membership in ANFIS	-	
		Epochs in ANFIS	80	
6	DT	Decision Tree	Entropy	
7	NB	Naïve Bayes Distribution	normal	
	GT 17 6	G	One-Against-One	
8	SVM	Strategy	One-Against-All	
	EL	Method in Ensemble Learning	AdaBoostM2	
9		NumTrained in Ensemble	100	
		LearnerNames in Ensemble	Tree	
	RNN	Hidden unit in RNN	100	
		Network AF in RNN	ReLU	
		Last LayerAF in RNN	Softmax	
10		Dropout in RNN	0.11	
10		Optimizer in RNN	Adam	
		MiniBatchSize in RNN	25	
		MaxEpochs in RNN	20	
		Loss Function in RNN	Cross-Entropy	
	LSTM	Hidden unit in LSTM	100	
		Network AF in LSTM	ReLU	
		Last Layer AF in LSTM	Softmax	
11		Dropout in LSTM	0.2	
11		Optimizer in LSTM	Adam	
		MiniBatchSize in LSTM	32	
		MaxEpochs in LSTM	30	
		Loss Function in LSTM	Cross-Entropy	

As evidenced by the results, the proposed model demonstrates impressive accuracy in differentiating among seven modulation classes, significantly outperforming traditional machine learning methods, ensemble learning approaches, and the DL-based RNN model. In the comparative analysis, the proposed model achieves an accuracy of 99.87% for AMR at -5 dB. This represents a significant improvement over the accuracy of the ten benchmark techniques evaluated. Specifically, the proposed architecture outperforms the MLP by 7.26%, the RBF by 29.13%, and the ANFIS by 34.03%. Additionally, the proposed algorithm surpasses the DT by 3.44%, NB by 24.65%, and KNN by 2.49%. It also achieves a notable advantage over the PNN by 3.32%, and the SVM configurations, i.e., SVM-OAO and SVM-OAA, by 1.77% and 1.84%, respectively. In comparison to ensemble learning, the proposed LSTM



Index	Algorithm	Accuracy %	Precision	F1 Score	Accuracy %	Precision	F1 Score	Time
		(0 dB)	(0 dB)	(0 dB)	(-5 dB)	(-5 dB)	(-5 dB)	(seconds)
1	MLP	100	0.9814	0.9813	93.11	0.9714	0.9712	3.06
2	RBF	99.33	0.8629	0.8620	77.33	0.7229	0.7222	5.41
3	ANFIS	90.24	0.8362	0.8420	74.56	0.6933	0.6789	4.73
4	DT	100	0.9943	0.9943	96.55	0.9686	0.9710	1.42
5	NB	100	0.9857	0.9857	80.11	0.7571	0.7490	7.59
6	KNN	100	0.9971	0.9971	97.44	0.9643	0.9647	5.01
7	PNN	100	0.9955	0.9954	96.66	0.9700	0.9700	7.63
8	SVM-OAO	100	0.9934	0.9937	98.13	0.9687	0.9691	23.79
9	SVM-OAA	100	0.9908	0.9911	98.07	0.9677	0.9689	13.08
10	Ensemble Learning	99.66	0.9957	0.9957	97.90	0.9543	0.9575	11.91
11	RNN	99.64	0.9947	0.9947	97.89	0.9729	0.9729	17.19
12	The Proposed Framework	100	0.9986	0.9985	99.87	0.9934	0.9942	17.27

TABLE 4. Performance metrics of various algorithms under different signal-to-noise ratios.

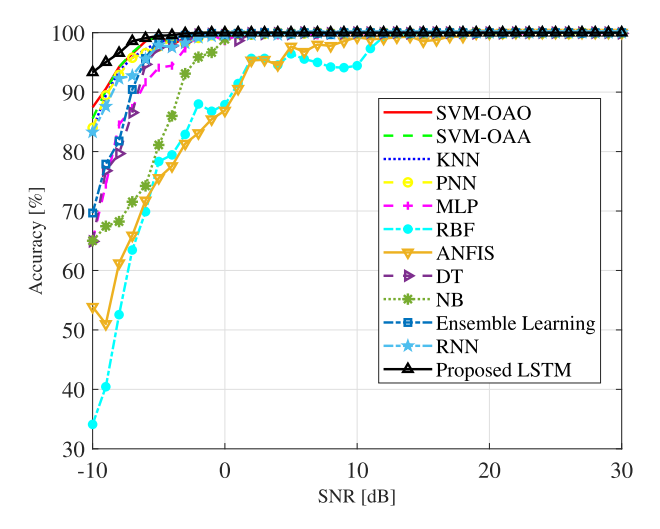


FIGURE 6. Comparative output illustrating the accuracy of the selected algorithms at different SNR levels.

technique achieves a remarkable enhancement of 2.01%. Furthermore, when benchmarked against the RNN, the proposed LSTM model delivers superior performance with a 2.02% improvement. These results underscore the superiority of the proposed approach in achieving higher accuracy in AMR tasks.

Furthermore, two additional graphs delineate the variations in accuracy and loss function across epochs, depicted in Figures 8 and 9. The accuracy graph demonstrates that exceptional performance is achieved shortly after the first epoch, with a steady upward trajectory in accuracy as the number of epochs increases. Concurrently, the loss function exhibits a consistent decline, indicating the efficacy of the learning process.

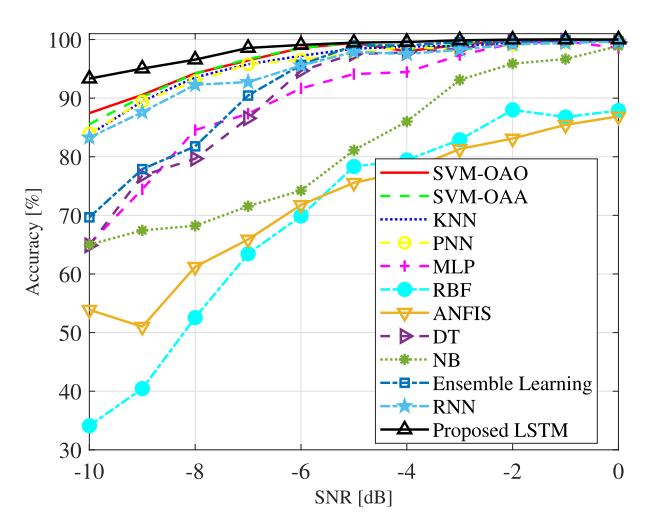


FIGURE 7. Detailed view of the comparative output, focusing on the accuracy of the selected algorithms at SNR levels between -10 and 0 dB.

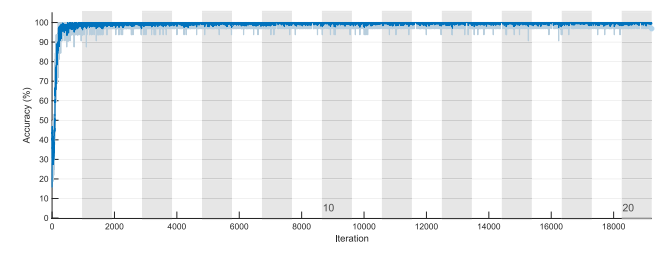


FIGURE 8. Accuracy performance chart during the training phase of the proposed model.

In addition, Table 5 provides a comprehensive comparison of the classification accuracy achieved by various methods across different modulation schemes. The results highlight



Reference	Modulation Schemes	Methodology	Accuracy (%)	
[66]	AM, BPSK, FSK, FM	CNN-based model with STFT	> 80% for SNRs $> -6$ dB	
[67]	ASK, PSK, FSK, QSK, QPSK,QFSK	Two-stage hybrid method	> 90% for SNRs > 0 dB	
[07]	ASK, ISK, ISK, QSK, QISK,QISK	combining STFT and CNN.		
[68]	BPSK, OPSK, 8-PSK, 16QAM	DNN-based model employing correlation coefficient	> 95% for SNRs > 0 dB	
[00]	Brok, Qrok, 6-rok, rogram	-based effective feature selection method	2 93 % for SNRs 2 0 dB	
[69]	BSPK, QPSK, 8-PSK, 16QAM	Maximum a posteriori probability (MAP)-	98% for SNR = $20 \text{ dB}$	
[05]	Born, Qron, o ron, rogram	DNN-based model	70 % 101 51 W = 20 UD	
[70]	8PSK, AM-DSB, AM-SSB, BPSK, CPFSK,	Time-frequency attention mechanism	85.7% for SNR = 10 dB	
[70]	GFSK, PAM4, QAM16, QAM64, QPSK	for CNN-based model	65.7 % 101 SIVK = 10 UB	
[71]	8PSK, AM-DSB, AM-SSB, BPSK, CPFSK,	Transfer learning-based model	> 70% for SNRs > 0 dB	
[/1]	GFSK, PAM4, QAM16, QAM64, QPSK	Transfer tearning-based model		
The Proposed	BASK, 4-ASK, BFSK, 4-FSK, BPSK, 4-PSK,	Optimized LSTM-based model employing adaptive	99.87% for SNR = $-5 \text{ dB}$	
Architecture	and 16-QAM.	temporal-spectral feature learning mechanism	99.07 % 101 SINK = -9 UD	

TABLE 5. Comparison of classification accuracy across various modulation schemes and methods.

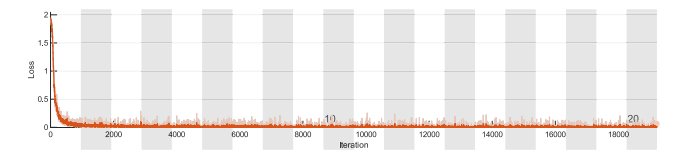


FIGURE 9. Performance chart of the loss function throughout the training phase of the proposed model.

the performance of several models, including CNN-based, DNN-based, and hybrid approaches, with accuracy ranging from 70% to 98%, depending on the modulation type and SNR. Notably, the proposed LSTM-based model achieves 99.87% accuracy at an SNR of -5 dB, demonstrating superior performance compared to the other methods. This comparison underscores the effectiveness of the proposed architecture in delivering high classification accuracy across a wide range of modulation schemes and challenging conditions.

Importantly, the DL algorithm presented herein circumvents the need for complex feature extraction processes, thereby offering significant operational efficiency and cost-effectiveness compared to conventional approaches. In summary, this work not only demonstrates the efficacy of DL techniques in AMR but also sets a new benchmark for future developments in the field. The findings advocate for a paradigm shift in how modulation types are classified, promising significant implications for the advancement of communication technologies.

Furthermore, to improve classification accuracy under phase noise conditions, the incorporation of constellation transformations, specifically the polar transformation of symbol coordinates in the IQ plane, is tested. This transformation, as suggested by Oikonomou et al. [28], aims to compensate for phase imperfections by adjusting the constellation points to mitigate phase distortions. The effects of this transformation are evaluated within the proposed

LSTM architecture, with simulations conducted to assess the impact on modulation recognition performance under various phase noise levels. The results indicated that while the polar transformation slightly improved robustness to phase imperfections, the performance gains are not substantial enough to surpass the original LSTM framework under typical conditions. The transformation helped reduce misclassifications in scenarios with significant phase noise, but its effect on overall accuracy is modest. These findings suggest that the integration of constellation transformations may be useful in handling phase imperfections, although it may need to be combined with other advanced techniques such as denoising algorithms or more sophisticated channel models for enhanced performance. This direction is proposed as a potential area for future research to further improve the robustness of AMR systems.

# C. LIMITATIONS AND FUTURE DIRECTIONS

The proposed LSTM-based architecture demonstrates outstanding performance in classification accuracy and robustness across diverse SNR conditions, reinforcing its potential for practical applications in AMR. However, it is important to acknowledge certain limitations inherent to the model and its deployment. Addressing these limitations not only underscores the transparency of this work but also provides a foundation for future advancements. These limitations, along with potential solutions and avenues for future research, are outlined below:

1) Computational Complexity: The proposed model comprises 100 hidden units, resulting in 840,400 trainable parameters, which ensures its ability to learn intricate temporal dependencies. However, this complexity introduces a computational burden during training and inference phases, particularly in resource-constrained environments. The reliance on



backpropagation through time (BPTT) for gradient optimization further accentuates this demand, potentially limiting its deployment in real-time or embedded systems. Accordingly, future investigations can explore lightweight alternatives, such as GRUs or low-rank LSTM models, which offer comparable performance with reduced computational overhead. Advanced techniques like model pruning, quantization, or knowledge distillation could also optimize the model's footprint while preserving accuracy.

- 2) Scalability to Diverse and Larger Datasets: The scalability of the model remains a critical challenge, especially when adapting to larger datasets or expanding the number of modulation types. The computational and memory demands grow significantly as dataset size and complexity increase, potentially introducing inefficiencies in handling real-world datasets or highly diverse modulation schemes. Distributed training frameworks, leveraging GPU clusters or cloudbased solutions, can mitigate scalability concerns. Incremental learning approaches, which allow the model to adapt to new modulation schemes without full retraining, could also be investigated. Such methods would significantly enhance the model's practicality and scalability in dynamic environments.
- 3) Adaptation to Real-World Scenarios: The experimental evaluation predominantly relies on synthetic datasets generated under controlled conditions. Real-world environments often introduce additional noise sources, interference, and dynamic signal characteristics that are absent from synthetic data. Such discrepancies could impact the model's performance when deployed in practical applications. Testing the model with real-world datasets, reflective of diverse operational environments, is a crucial next step. Transfer learning or domain adaptation techniques could further enhance the model's robustness to real-world variability. Additionally, designing preprocessing pipelines tailored to real-world challenges could significantly improve performance.

#### VI. CONCLUSION

This paper introduces an innovative DL architecture that significantly advances the field of AMR. The model leverages LSTM networks to automate feature extraction during the classification process, marking a departure from traditional methods that rely heavily on manual feature engineering. This approach not only simplifies the workflow but also enhances the accuracy and efficiency of modulation recognition tasks. Experimental results demonstrate that the proposed model achieves exceptional performance, outperforming traditional algorithms, an ensemble learning method, and the DL-based RNN model. Specifically, the model delivers a remarkable 3.89% increase in accuracy at an SNR of -2 dB compared to the best-performing conventional method, highlighting its robustness and ability to handle

noise and variability in real-world scenarios. Furthermore, when compared to the RNN, the proposed LSTM model achieves a performance gain of 1.73%, further emphasizing its superiority in tackling AMR challenges. The use of the Adam optimization algorithm further enhances the model's performance, highlighting its adaptability and effectiveness. Looking ahead, future research will explore the integration of evolutionary algorithms and the application of advanced DL architectures, including attention mechanisms, to further improve classification accuracy across diverse datasets such as RadioML 2016.10a, RadioML 2018.01A, and HisarMod 2019.1. Additionally, we aim to investigate the performance of the proposed framework within the context of emerging communication technologies, specifically B5G and 6G wireless networks. This will involve considering various communication channels and conditions to ensure the model's scalability and relevance in next-generation wireless systems.

#### **REFERENCES**

- [1] F. Wen, X. Zhang, and Z. Zhang, "CRBs for direction-of-departure and direction-of-arrival estimation in collocated MIMO radar in the presence of unknown spatially coloured noise," *IET Radar, Sonar Navigat.*, vol. 13, no. 4, pp. 530–537, Apr. 2019. [Online]. Available: https://ietresearch.onlinelibrary.wiley.com/doi/abs/10.1049/iet-rsn.2018.5386
- [2] S. Ansari and K. Alnajjar, "Adaptive modulation and coding: A brief review of the literature," *Int. J. Commun. Antenna Propag.*, vol. 13, no. 1, pp. 43–54, Feb. 2023.
- [3] A. K. Nandi and E. E. Azzouz, "Algorithms for automatic modulation recognition of communication signals," *IEEE Trans. Commun.*, vol. 46, no. 4, pp. 431–436, Apr. 1998.
- [4] S. Ansari, K. A. Alnajjar, S. Abdallah, and M. Saad, "Automatic digital modulation recognition based on machine learning algorithms," in *Proc. Int. Conf. Commun., Comput., Cybersecurity, Informat. (CCCI)*, Nov. 2020, pp. 1–6.
- [5] B. Jdid, K. Hassan, I. Dayoub, W. H. Lim, and M. Mokayef, "Machine learning based automatic modulation recognition for wireless communications: A comprehensive survey," *IEEE Access*, vol. 9, pp. 57851–57873, 2021.
- [6] S. Ansari, K. A. Alnajjar, M. Saad, S. Abdallah, and A. A. El-Moursy, "Automatic digital modulation recognition based on geneticalgorithm-optimized machine learning models," *IEEE Access*, vol. 10, pp. 50265–50277, 2022.
- [7] K. A. Alnajjar, S. Ghunaim, and S. Ansari, "Automatic modulation classification in deep learning," in *Proc. 5th Int. Conf. Commun., Signal Process., Appl. (ICCSPA)*, Dec. 2022, pp. 1–5.
- [8] D. Zhang, Y. Lu, Y. Li, W. Ding, B. Zhang, and J. Xiao, "Frequency learning attention networks based on deep learning for automatic modulation classification in wireless communication," *Pattern Recognit.*, vol. 137, May 2023, Art. no. 109345. [Online]. Available: https://www.sciencedirect.com/science/article/pii/S0031320323000468
- [9] Q. Zhou, X. Jing, Y. He, Y. Cui, M. Kadoch, and M. Cheriet, "LSTM-based automatic modulation classification," in *Proc. IEEE Int. Symp. Broadband Multimedia Syst. Broadcast. (BMSB)*, Oct. 2020, pp. 1–4.
- [10] R. Li, L. Li, S. Yang, and S. Li, "Robust automated VHF modulation recognition based on deep convolutional neural networks," *IEEE Commun. Lett.*, vol. 22, no. 5, pp. 946–949, May 2018.
- [11] S. Ansari, K. A. Alnajjar, S. Mahmoud, R. Alabdan, H. Alzaabi, M. Alkaabi, and A. Hussain, "Blind source separation based on genetic algorithm-optimized multiuser kurtosis," in *Proc. 46th Int. Conf. Telecommun. Signal Process. (TSP)*, Jul. 2023, pp. 164–171.
- [12] A.-K. Hamid and S. Ansari, "Optimal placement of grid-connected wind farms based on artificial intelligence techniques," in Proc. Adv. Sci. Eng. Technol. Int. Conf. (ASET), Feb. 2022, pp. 1–8.
- [13] S. Ansari and A. B. Nassif, "A comprehensive study of regression analysis and the existing techniques," in *Proc. Adv. Sci. Eng. Tech*nol. Int. Conf. (ASET), Feb. 2022, pp. 1–10.



- [14] S. Ansari, K. A. Alnajjar, T. Khater, S. Mahmoud, and A. Hussain, "A robust hybrid neural network architecture for blind source separation of speech signals exploiting deep learning," *IEEE Access*, vol. 11, pp. 100414–100437, 2023.
- [15] T. O'Shea and J. Hoydis, "An introduction to deep learning for the physical layer," *IEEE Trans. Cogn. Commun. Netw.*, vol. 3, no. 4, pp. 563–575, Dec. 2017.
- [16] Y. Lin, Y. Tu, Z. Dou, and Z. Wu, "The application of deep learning in communication signal modulation recognition," in *Proc. IEEE/CIC* Int. Conf. Commun. China (ICCC), Oct. 2017, pp. 1–5.
- [17] Y. Zeng, M. Zhang, F. Han, Y. Gong, and J. Zhang, "Spectrum analysis and convolutional neural network for automatic modulation recognition," *IEEE Wireless Commun. Lett.*, vol. 8, no. 3, pp. 929–932, Jun. 2019.
- [18] S. Huang, L. Chai, Z. Li, D. Zhang, Y. Yao, Y. Zhang, and Z. Feng, "Automatic modulation classification using compressive convolutional neural network," *IEEE Access*, vol. 7, pp. 79636–79643, 2019.
- [19] S. Huang, Y. Jiang, Y. Gao, Z. Feng, and P. Zhang, "Automatic modulation classification using contrastive fully convolutional network," *IEEE Wireless Commun. Lett.*, vol. 8, no. 4, pp. 1044–1047, Aug. 2019.
- [20] Y. Wang, M. Liu, J. Yang, and G. Gui, "Data-driven deep learning for automatic modulation recognition in cognitive radios," *IEEE Trans. Veh. Technol.*, vol. 68, no. 4, pp. 4074–4077, Apr. 2019.
- [21] C. Szegedy, W. Liu, Y. Jia, P. Sermanet, S. Reed, D. Anguelov, D. Erhan, V. Vanhoucke, and A. Rabinovich, "Going deeper with convolutions," in *Proc. IEEE Conf. Comput. Vis. Pattern Recognit. (CVPR)*, Jun. 2015, pp. 1–9.
- [22] N. E. West and T. O'Shea, "Deep architectures for modulation recognition," in *Proc. IEEE Int. Symp. Dyn. Spectr. Access Netw. (DySPAN)*, Mar. 2017, pp. 1–6.
- [23] B. Xu, U. A. Bhatti, H. Tang, J. Yan, S. Wu, N. Sarhan, E. M. Awwad, M. S. Syam, and Y. Y. Ghadi, "Towards explainability for AI-based edge wireless signal automatic modulation classification," *J. Cloud Comput.*, vol. 13, no. 1, p. 10, Jan. 2024, doi: 10.1186/s13677-024-00590-3.
- [24] G. Gui, H. Huang, Y. Song, and H. Sari, "Deep learning for an effective nonorthogonal multiple access scheme," *IEEE Trans. Veh. Technol.*, vol. 67, no. 9, pp. 8440–8450, Sep. 2018.
- [25] Q. Zheng, X. Tian, L. Yu, A. Elhanashi, and S. Saponara, "Recent advances in automatic modulation classification technology: Methods, results, and prospects," *Int. J. Intell. Syst.*, vol. 2025, no. 1, Jan. 2025. [Online]. Available: https://onlinelibrary.wiley.com/doi/abs/10.1155/int/4067323
- [26] L. Guo, Y. Wang, Y. Liu, Y. Lin, H. Zhao, and G. Gui, "Ultralight convolutional neural network for automatic modulation classification in Internet of unmanned aerial vehicles," *IEEE Internet Things J.*, vol. 11, no. 11, pp. 20831–20839, Jun. 2024.
- [27] B. Xu, C. Luo, H. Tang, U. A. Bhatti, X. Wang, and W. Jiang, "Advancing transparency in AI-based automatic modulation classification," in *Proc. IEEE/CIC Int. Conf. Commun. China (ICCC)*, Aug. 2024, pp. 2065–2070.
- [28] T. K. Oikonomou, N. G. Evgenidis, D. G. Nixarlidis, D. Tyrovolas, S. A. Tegos, P. D. Diamantoulakis, P. G. Sarigiannidis, and G. K. Karagiannidis, "CNN-based automatic modulation classification under phase imperfections," *IEEE Wireless Commun. Lett.*, vol. 13, no. 5, pp. 1508–1512, May 2024.
- [29] H. Huang, Y. Song, J. Yang, G. Gui, and F. Adachi, "Deep-learning-based millimeter-wave massive MIMO for hybrid precoding," *IEEE Trans. Veh. Technol.*, vol. 68, no. 3, pp. 3027–3032, Mar. 2019.
- [30] M. Liu, T. Song, J. Hu, J. Yang, and G. Gui, "Deep learning-inspired message passing algorithm for efficient resource allocation in cognitive radio networks," *IEEE Trans. Veh. Technol.*, vol. 68, no. 1, pp. 641–653, Jan. 2019.
- [31] C.-K. Wen, W.-T. Shih, and S. Jin, "Deep learning for massive MIMO CSI feedback," *IEEE Wireless Commun. Lett.*, vol. 7, no. 5, pp. 748–751, Oct. 2018.
- [32] M. Liu, T. Song, and G. Gui, "Deep cognitive perspective: Resource allocation for NOMA-based heterogeneous IoT with imperfect SIC," *IEEE Internet Things J.*, vol. 6, no. 2, pp. 2885–2894, Apr. 2019.
- [33] M. A. Abdel-Moneim, W. El-Shafai, N. Abdel-Salam, E. M. El-Rabaie, and F. E. A. El-Samie, "A survey of traditional and advanced automatic modulation classification techniques, challenges, and some novel trends," *Int. J. Commun. Syst.*, vol. 34, no. 10, p. 4762, Jul. 2021. [Online]. Available: https://onlinelibrary.wiley.com/doi/abs/10.1002/dac.4762

- [34] S. T. H. Chahil, M. Zakwan, K. Khan, and A. Fazil, "Performance analysis of different signal representations and optimizers for CNN based automatic modulation classification," *Wireless Pers. Commun.*, vol. 139, no. 4, pp. 2503–2528, Dec. 2024, doi: 10.1007/s11277-024-11722-y.
- [35] T. J. O'Shea, J. Corgan, and T. C. Clancy, "Unsupervised representation learning of structured radio communication signals," in *Proc. 1st Int. Workshop Sens.*, *Process. Learn. Intell. Mach. (SPLINE)*, Jul. 2016, pp. 1–5.
- [36] T. J. O'Shea, J. Corgan, and T. C. Clancy, "Convolutional radio modulation recognition networks," 2016, arXiv:1602.04105.
- [37] T. J. O'Shea, J. Corgan, and T. C. Clancy, "Convolutional radio modulation recognition networks," in *Engineering Applications of Neural Networks*, C. Jayne and L. Iliadis, Eds., Cham, Switzerland: Springer, 2016, pp. 213–226.
- [38] M. Kulin, T. Kazaz, I. Moerman, and E. De Poorter, "End-to-end learning from spectrum data: A deep learning approach for wireless signal identification in spectrum monitoring applications," *IEEE Access*, vol. 6, pp. 18484–18501, 2018.
- [39] K. Yashashwi, A. Sethi, and P. Chaporkar, "A learnable distortion correction module for modulation recognition," *IEEE Wireless Commun. Lett.*, vol. 8, no. 1, pp. 77–80, Feb. 2019.
- [40] D. Wang, M. Zhang, Z. Li, J. Li, M. Fu, Y. Cui, and X. Chen, "Modulation format recognition and OSNR estimation using CNN-based deep learning," *IEEE Photon. Technol. Lett.*, vol. 29, no. 19, pp. 1667–1670, Oct. 1, 2017.
- [41] S. Peng, H. Jiang, H. Wang, H. Alwageed, Y. Zhou, M. M. Sebdani, and Y.-D. Yao, "Modulation classification based on signal constellation diagrams and deep learning," *IEEE Trans. Neural Netw. Learn. Syst.*, vol. 30, no. 3, pp. 718–727, Mar. 2019.
- [42] Z. Zhang, C. Wang, C. Gan, S. Sun, and M. Wang, "Automatic modulation classification using convolutional neural network with features fusion of SPWVD and BJD," *IEEE Trans. Signal Inf. Process. Over Netw.*, vol. 5, no. 3, pp. 469–478, Sep. 2019.
- [43] T. K. Oikonomou, S. A. Tegos, D. Tyrovolas, P. D. Diamantoulakis, and G. K. Karagiannidis, "On the error analysis of hexagonal-QAM constellations," *IEEE Commun. Lett.*, vol. 26, no. 8, pp. 1764–1768, Aug. 2022.
- [44] S. Rajendran, W. Meert, D. Giustiniano, V. Lenders, and S. Pollin, "Deep learning models for wireless signal classification with distributed lowcost spectrum sensors," *IEEE Trans. Cogn. Commun. Netw.*, vol. 4, no. 3, pp. 433–445, Sep. 2018.
- [45] N. Chakravarty, M. Dua, and S. Dua, "Automatic modulation classification using amalgam CNN-LSTM," in *Proc. IEEE Radio Antenna Days Indian Ocean (RADIO)*, May 2023, pp. 1–2.
- [46] M. M. Elsagheer and S. M. Ramzy, "A hybrid model for automatic modulation classification based on residual neural networks and long short term memory," *Alexandria Eng. J.*, vol. 67, pp. 117–128, Mar. 2023. [Online]. Available: https://www.sciencedirect.com/science/article/pii/S1110016822005488
- [47] Z. Zhang, H. Luo, C. Wang, C. Gan, and Y. Xiang, "Automatic modulation classification using CNN-LSTM based dual-stream structure," *IEEE Trans. Veh. Technol.*, vol. 69, no. 11, pp. 13521–13531, Nov. 2020.
- [48] Z. Ke and H. Vikalo, "Real-time radio technology and modulation classification via an LSTM auto-encoder," *IEEE Trans. Wireless Commun.*, vol. 21, no. 1, pp. 370–382, Jan. 2022.
- [49] F. Jia, Y. Yang, J. Zhang, and Y. Yang, "A hybrid attention mechanism for blind automatic modulation classification," *Trans. Emerg. Telecom-mun. Technol.*, vol. 33, no. 7, p. 4503, Jul. 2022. [Online]. Available: https://onlinelibrary.wiley.com/doi/abs/10.1002/ett.4503
- [50] D. Wang, M. Lin, X. Zhang, Y. Huang, and Y. Zhu, "Automatic modulation classification based on CNN-transformer graph neural network," *Sensors*, vol. 23, no. 16, p. 7281, Aug. 2023. [Online]. Available: https://www.mdpi.com/1424-8220/23/16/7281
- [51] Z. Ma, S. Fang, Y. Fan, G. Li, and H. Hu, "An efficient and lightweight model for automatic modulation classification: A hybrid feature extraction network combined with attention mechanism," *Electronics*, vol. 12, no. 17, p. 3661, Aug. 2023. [Online]. Available: https://www.mdpi.com/2079-9292/12/17/3661
- [52] N. D. Indira and M. V. G. Rao, "Deep learning CNN-based hybrid extreme learning machine with bagging classifier for automatic modulation classification," *Int. J. Intell. Syst. Appl. Eng.*, vol. 10, no. 2s, pp. 134–141, Dec. 2022. [Online]. Available: https://www.ijisae.org/index.php/IJISAE/article/view/2373



- [53] L. Li, Y. Zhu, and Z. Zhu, "Automatic modulation classification using ResNeXt-GRU with deep feature fusion," *IEEE Trans. Instrum. Meas.*, vol. 72, pp. 1–10, 2023.
- [54] S. Ying, S. Huang, S. Chang, Z. Yang, Z. Feng, and N. Guo, "A convolutional and transformer based deep neural network for automatic modulation classification," *China Commun.*, vol. 20, no. 5, pp. 135–147, May 2023.
- [55] S.-H. Kim, C.-B. Moon, J.-W. Kim, and D.-S. Kim, "A hybrid deep learning model for automatic modulation classification," *IEEE Wireless Commun. Lett.*, vol. 11, no. 2, pp. 313–317, Feb. 2022.
- [56] B. Liu, Q. Zheng, H. Wei, J. Zhao, H. Yu, Y. Zhou, F. Chao, and R. Ji, "Deep hybrid transformer network for robust modulation classification in wireless communications," *Knowl.-Based Syst.*, vol. 300, Sep. 2024, Art. no. 112191. [Online]. Available: https://www.sciencedirect.com/science/article/pii/S0950705124008256
- [57] K. Hassan, I. Dayoub, W. Hamouda, and M. Berbineau, "Automatic modulation recognition using wavelet transform and neural networks in wireless systems," *EURASIP J. Adv. Signal Process.*, vol. 2010, no. 1, pp. 1–13, Dec. 2010.
- [58] S. Hassanpour, A. M. Pezeshk, and F. Behnia, "Automatic digital modulation recognition based on novel features and support vector machine," in *Proc. 12th Int. Conf. Signal-Image Technol. Internet-Based* Syst. (SITIS), Nov. 2016, pp. 172–177.
- [59] F. F. Liedtke, "Computer simulation of an automatic classification procedure for digitally modulated communication signals with unknown parameters," Signal Process., vol. 6, no. 4, pp. 311–323, Aug. 1984. [Online]. Available: https://www.sciencedirect.com/ science/article/pii/016516848490063X
- [60] M. P. DeSimio and G. E. Prescott, "Adaptive generation of decision functions for classification of digitally modulated signals," in *Proc. IEEE Nat. Aerosp. Electron. Conf.*, vol. 3, May 1988, pp. 1010–1014.
- [61] S.-Z. Hsue and S. S. Soliman, "Automatic modulation classification using zero crossing," *IEE Proc. F Radar Signal Process.*, vol. 137, no. 6, pp. 459–464, 1990. [Online]. Available: https://digitallibrary.theiet.org/content/journals/10.1049/ip-f-2.1990.0066
- [62] X. Zhang, J. Sun, and X. Zhang, "Automatic modulation classification based on novel feature extraction algorithms," *IEEE Access*, vol. 8, pp. 16362–16371, 2020.
- [63] K. Liao, Y. Zhao, J. Gu, Y. Zhang, and Y. Zhong, "Sequential convolutional recurrent neural networks for fast automatic modulation classification," *IEEE Access*, vol. 9, pp. 27182–27188, 2021.
- [64] A. Sherstinsky, "Fundamentals of recurrent neural network (RNN) and long short-term memory (LSTM) network," *Phys. D, Nonlinear Phenomena*, vol. 404, Mar. 2020, Art. no. 132306. [Online]. Available: https://www.sciencedirect.com/science/article/pii/S0167278919305974
- [65] S. Hassanpour, A. M. Pezeshk, and F. Behnia, "A robust algorithm based on wavelet transform for recognition of binary digital modulations," in *Proc. 38th Int. Conf. Telecommun. Signal Process. (TSP)*, Jul. 2015, pp. 508–512.
- [66] Q. Zhang, Z. Xu, and P. Zhang, "Modulation scheme recognition using convolutional neural network," *J. Eng.*, vol. 2019, no. 23, pp. 9075–9078, Dec. 2019. [Online]. Available: https://ietresearch.onlinelibrary.wiley. com/doi/abs/10.1049/joe.2018.9188
- [67] N. Daldal, Z. Cömert, and K. Polat, "Automatic determination of digital modulation types with different noises using convolutional neural network based on time-frequency information," *Appl. Soft Comput.*, vol. 86, Jan. 2020, Art. no. 105834. [Online]. Available: https://www. sciencedirect.com/science/article/pii/S1568494619306155
- [68] S. H. Lee, K.-Y. Kim, and Y. Shin, "Effective feature selection method for deep learning-based automatic modulation classification scheme using higher-order statistics," *Appl. Sci.*, vol. 10, no. 2, p. 588, Jan. 2020. [Online]. Available: https://www.mdpi.com/2076-3417/10/ 2/588
- [69] S. Hu, Y. Pei, P. P. Liang, and Y.-C. Liang, "Deep neural network for robust modulation classification under uncertain noise conditions," *IEEE Trans. Veh. Technol.*, vol. 69, no. 1, pp. 564–577, Jan. 2020.
- [70] S. Lin, Y. Zeng, and Y. Gong, "Learning of time-frequency attention mechanism for automatic modulation recognition," *IEEE Wireless Commun. Lett.*, vol. 11, no. 4, pp. 707–711, Apr. 2022.
- [71] W. Lin, D. Hou, J. Huang, L. Li, and Z. Han, "Transfer learning for automatic modulation recognition using a few modulated signal samples," *IEEE Trans. Veh. Technol.*, vol. 72, no. 9, pp. 12391–12395, Sep. 2023.



**SAM ANSARI** received the B.Sc. degree in telecommunication engineering from Canadian University Dubai, Dubai, United Arab Emirates, the M.Sc. degree in electrical and computer engineering from Abu Dhabi University, Abu Dhabi, United Arab Emirates, and the Ph.D. degree in electrical and computer engineering from the University of Sharjah, Sharjah, United Arab Emirates. He is currently a Postdoctoral Research Associate with the Research Institute

of Science and Engineering, University of Sharjah. His research interests include wireless communications, signal and image processing, molecular communication, artificial intelligence, machine learning, and renewable energy.



**SOLIMAN MAHMOUD** (Senior Member, IEEE) was born in Cairo, Egypt, in 1971. He received the B.Sc. (Hons.), M.Sc., and Ph.D. degrees from the Electronics and Communications Department, Cairo University, Egypt, in 1994, 1996, and 1999, respectively. He is currently a Professor with the Electrical Engineering Department, University of Sharjah, Sharjah, United Arab Emirates. From September 2023 to October 2024, he was the Vice Chancellor for Academic Affairs, University of

Khorfakkan, Khorfakkan, United Arab Emirates, while on leave from his position with the University of Sharjah. He has been a Professor with the Electrical Engineering Department, Fayoum University, Fayoum, Egypt, since 2010. He has supervised four Ph.D. students, 17 M.Sc. students, and more than 50 senior design projects. He is actively engaged in scholarly research and has authored or co-authored more than 220 journal and conference publications since joining academia, in 1996. His research accomplishments include receiving "The German-Egyptian Research Fund" Grant, which funded the project "Design of CMOS Field Programmable Analog Array and Its Applications," carried out in collaboration with Ulm Microelectronics Institute, Ulm University, Germany. His publications have garnered more than 2500 citations and his Google Scholar H-index is 27 (Scopus H-index is 24). He has published six refereed research books. His research interests include mixed analog/digital integrated electronic circuit (IC) design, including mixed-mode (voltage/current) analog circuits, mixed (analog/digital) programmable CMOS electronics systems, biomedical circuits, field-programmable analog arrays (FPGAs), and multi-standard wireless receiver design. He received the Science Prize in Advanced Engineering Technology from the Academy of Scientific Research and Technology, Ministry of Higher Education, Cairo, in 2005. He also received the Distinguished Research Award from the University of Sharjah, from 2011 to 2012 and from 2014 to 2015.



**SOHAIB MAJZOUB** (Senior Member, IEEE) received the Ph.D. degree from The University of British Columbia, Canada, in 2010. He worked for two years as an Assistant Professor with American University in Dubai, Dubai, United Arab Emirates, and three years with King Saud University, up until 2015. He is currently an Associate Professor with the University of Sharjah, United Arab Emirates, and a Faculty Member with the Electrical Engineering Department. His research interests include

VLSI/embedded systems design, low power manycore design, memristor, and random number generation and encryption. He is a member of the IEEE Computer Society, the Solid State Society, and the Circuits and Systems Member.





**EQAB ALMAJALI** (Member, IEEE) received the B.Sc. degree (Hons.) from Mu'tah University, Jordan, and the M.A.Sc. and Ph.D. degrees (Hons.) in electrical engineering from the University of Ottawa, Ottawa, ON, Canada, in 2010 and 2014, respectively. He has been an Associate Professor with the Electrical Engineering Department, University of Sharjah, since January 2024. Prior to that, he was an Assistant Professor with the Electrical Engineering Department for five years.

He is the author of more than 80 technical publications and two book chapters. His current research interests include the application of AI in antennas and sensors design, millimeter-wave MIMO antennas, reconfigurable antennas, RF passive and active sensors, THz antennas, and wireless power transfer. He received the prestigious Canadian National Science and Engineering Research Council (NSERC) Postdoctoral Fellowship for his Research Excellence, in 2014, and the NSERC-PGS Scholarship during his Ph.D. studies, in 2012.



**TALAL BONNY** received the M.Sc. degree from the Technical University of Braunschweig, Germany, in 2002, and the Ph.D. degree from Karlsruhe Institute of Technology, Germany, in 2009. He is currently an Associate Professor with the Department of Computer Engineering, College of Computing and Informatics, University of Sharjah, where he has been a Faculty Member, since 2013. His current research interests include embedded systems, hardware digital design, image

processing, chaotic oscillator realizations, secure communication systems, AI and machine learning, and bioinformatics. He served as a reviewer/a TPC member in many IEEE/ACM journals/conferences. He was the Session Chair of the IEEE Conference on Advances in Artificial Intelligence.

0 0 0



ANWAR JARNDAL (Senior Member, IEEE) received the Ph.D. degree in electrical engineering from the University of Kassel, Kassel, Germany, in 2006. He was a Postdoctoral Fellow with École de Technologie Supérieure (ETS), Quebec University, Canada. He is currently a Full Professor with the Department of Electrical Engineering, University of Sharjah. He has published more than 140 internationally peer-reviewed publications. He was also classified as one of the World's Top

2% Scientists (Stanford University), in 2020. His research interests include active device modeling, measurements and characterization techniques, power amplifier design, low-noise amplifier design, active sensors, local and global optimizations, artificial neural networks, machine learning, fuzzy logic, radio channel modeling, and wireless power transfer. He is serving as a reviewer for more than 25 international journals. He received the Annual Incentives Award for the Distinguished Faculty in Scientific Research from the University of Sharjah.